

MODELING OF INITIAL GEOMETRICAL IMPERFECTIONS IN STABILITY ANALYSIS OF THIN-WALLED STRUCTURES

KATARZYNA RZESZUT
ANDRZEJ GARSTECKI

*Poznań University of Technology, Institute of Structural Engineering, Poznań, Poland
e-mail: katarzyna.rzeszut@put.poznan.pl*

Imperfections are modeled using actual values measured in situ. The method proposed in the paper is based on the concept of developing the imperfections in series of eigenmodes, using a limited number of most critical eigenmodes. Error minimization of this representation is performed. The method is applied to the nonlinear stability analysis of structures made of steel thin-walled cold-formed sigma profiles. FEM with shell elements and the Riks method are used. Numerical examples illustrate the influence of initial imperfections on post buckling behavior of structures.

Key words: stability analysis, initial geometric imperfections, thin-walled beams, stability of cold-formed bars

1. Introduction

In the case of cold-formed steel members, initial geometric imperfections can significantly influence stability response, because usually a local buckling appears closed to the global one. There are several studies which consider different types of geometric imperfections and ways of their introduction into a numerical model. One way of taking initial geometric imperfections into account, which dominates in design codes, is to induce them by applying an appropriate pattern of additional loading. However, it works well only for the global type of imperfections, e.g. in the case of multistory frames with columns exhibiting deviations from the vertical direction. In the case of local sectional imperfections, it seems reasonable to introduce perturbed geometry by measured values of imperfections. However, this procedure can be tedious when the finite element method is used. Moreover, it is not a general procedure since it can be applied

only to those members for which the imperfections have been measured. An alternative method of introduction of imperfections, widely discussed in the literature, is stochastic generation of the imperfection signal (Laubscher, 2004). Another approach to the stability analysis of imperfect structures is based on the concept of sensitivity analysis. The potential of sensitivity analysis of thin walled beams and columns accounting for nonlinear effects was discussed in Chróścielewski *et al.* (2006), Szymczak (2006). However, keeping in mind that eigenmodes represent the most dangerous shapes of imperfections, the introduction of imperfections in the form of eigenmodes (Dubina *et al.*, 2001) can be considered as a classical approach. It would be reasonable to treat the perturbation in the geometry as a linear superposition of buckling modes with scale factors computed from measurements (Fang and Pekoz, 2001; Garstecki *et al.*, 2002; Lechner and Pircher, 2005). Therefore, proper modeling of imperfections, which correspond with real imperfections, can play an important role in structural analysis and design.

In the paper, the problem of modeling the initial geometrical imperfections basing on actual imperfections measured in situ is discussed and the methods presented in Garstecki *et al.* (2002) and Kąkol *et al.* (2002) are further developed. The present approach is based on the concept of developing the imperfections in series of eigenmodes computed from a linear stability problem. A limited number of most critical eigenmodes is used. The coefficients in the series are evaluated using actual imperfections (Garstecki *et al.*, 2002), accounting for Gauss probability factors and implementing error minimization in the approximation. We start from simple examples illustrating the method and demonstrating its accuracy. Next, the method is applied to stability analysis of structures made of steel thin-walled cold-formed sigma profiles. The Riks method is used for solution of the nonlinear stability problem.

2. Method of modeling the imperfection

Notation

- N – total number of degrees of freedom in FEM model
- r – consecutive number of displacement in FEM model, $r = 1, \dots, N$
- n – total number of eigenmodes in approximation
- i – consecutive number of eigenmode, $i = 1, \dots, n$
- m – total number of measurements of imperfections

- k – consecutive number of measurement of imperfection, $k = 1, \dots, m$
- \mathbf{u} – N -dimensional displacement vector of actual imperfections (unknown)
- \mathbf{u}_i – N -dimensional displacement vector representing i -th eigenmode
- α – n -dimensional vector of scale factors
- \mathbf{v} – m -dimensional displacement vector of measured imperfections
- \mathbf{v}_i – m -dimensional displacement vector similar to \mathbf{v} but extracted from \mathbf{u}_i

The initial geometric imperfections are introduced by perturbations in the "perfect" geometry. In a continuous formulation, the imperfection can be written in the form

$$\tilde{u}(\alpha_i, x) = \sum_{i=1}^n \alpha_i u_i(x) \tag{2.1}$$

where \mathbf{x} is the coordinate vector, $u_i(x)$ are test functions and α_i are scale factors. Assume the test functions in the form of buckling modes obtained from the linear stability problem and associated with n lowest eigenvalues. Since we apply FEM, the buckling modes $u_i(x)$ and similarly $\tilde{u}(x)$ have the form of N -dimensional displacement vectors \mathbf{u}_i , where N is the number of DOF in the FEM model. In FEM $\tilde{\mathbf{u}}, \mathbf{u}_i \in \mathcal{R}^N$, hence Eq. (2.1) takes the form

$$\tilde{\mathbf{u}} = [\tilde{u}_r] = \sum_{i=1}^n \alpha_i \mathbf{u}_i = \left[\sum_{i=1}^n \alpha_i U_{ir} \right]^T = \mathbf{U}^T \alpha \tag{2.2}$$

where U_{ir} denotes the displacement r of eigenmode i . Hence the dimensions of \mathbf{U} are $n \times N$. Note, that in the approximation (Eqs. (2.1) and (2.2)) we used only n eigenvectors, where $n \ll N$. Usually, it is recommended to use those ones, which are associated with the smallest eigenvalues. However, the assumed set of eigenvalues and eigenmodes must contain those local and global modes which are similar to the shape of real imperfections. Otherwise, linear combinations of the limited number of eigenmodes will not be able to capture the real imperfection pattern.

Our task is to find the factors α_i which minimize the error

$$\mathbf{u} - \tilde{\mathbf{u}} = \mathbf{u} - \mathbf{U}^T \alpha \rightarrow \min_{\alpha} \quad \mathbf{u}, \tilde{\mathbf{u}} \in \mathcal{R}^N \tag{2.3}$$

However, we do not know the real imperfections \mathbf{u} in the space \mathcal{R}^N , because the measurements of initial geometry in situ provide only m displacements representing the imperfections. Usually, $m \ll N$ and $m > n$. Denote the consecutive displacements specifying the measured imperfection by v_k and the

imperfection displacement vector by $\mathbf{v} = [v_k]$, $\mathbf{v} \in \mathcal{R}^m$. The error, Eq. (2.3), can be evaluated using these m displacements, only.

Let the FEM mesh and the nodal displacements are introduced to stability analysis in such a form that the measured imperfection displacements v_k coincide with respective nodal displacements u_r , and hence there is a unique mapping $r \rightarrow k$

$$r \rightarrow k \quad (2.4)$$

Using Eq. (2.4), we can extract the respective displacements k of the eigenmode i , namely a component V_{ik} of the N -dimensional matrix of eigenmodes U_{ir} . The rows i of the matrix V_{ik} represent the vectors \mathbf{v}_i , which will be used as test functions in error minimization of the approximation.

Now, the approximation of the measured imperfection displacement vector \mathbf{v} takes the form

$$\tilde{\mathbf{v}} = [\tilde{v}_k] = \sum_{i=1}^n \alpha_i \mathbf{v}_i = \left[\sum_{i=1}^n \alpha_i V_{ik} \right]^\top = \mathbf{V}^\top \boldsymbol{\alpha} \quad (2.5)$$

The error of approximation can now be represented by the vector $\boldsymbol{\varepsilon}$ in the space \mathcal{R}^m

$$\boldsymbol{\varepsilon} = \mathbf{v} - \sum_{i=1}^n \alpha_i \mathbf{v}_i = \mathbf{v} - \mathbf{V}^\top \boldsymbol{\alpha} \rightarrow \min_{\boldsymbol{\alpha}} \quad \begin{array}{l} \boldsymbol{\varepsilon}, \mathbf{v} \in \mathcal{R}^m \\ \boldsymbol{\alpha} \in \mathcal{R}^n \end{array} \quad (2.6)$$

Following the Galerkin concept, we assume optimal $\boldsymbol{\alpha}$, when it makes $\boldsymbol{\varepsilon}$ orthogonal to all test functions \mathbf{v}_i , namely

$$\boldsymbol{\varepsilon} \mathbf{v}_i = 0 \quad (2.7)$$

where dot denotes scalar product. Introducing (2.6) into (2.7), we obtain

$$\left(\mathbf{v} - \sum_{i=1}^n \alpha_i \mathbf{v}_i \right) \mathbf{v}_j = 0 \quad (2.8)$$

The matrix form of (2.8) is

$$\mathbf{V} \mathbf{v} - \mathbf{V} \mathbf{V}^\top \boldsymbol{\alpha} = \mathbf{0} \quad \text{or} \quad \mathbf{V} \mathbf{V}^\top \boldsymbol{\alpha} = \mathbf{V} \mathbf{v} \quad (2.9)$$

Introducing

$$\mathbf{A} = \mathbf{V} \mathbf{V}^\top \quad \text{and} \quad \mathbf{b} = \mathbf{V} \mathbf{v} \quad (2.10)$$

we obtain

$$\mathbf{A} \boldsymbol{\alpha} = \mathbf{b} \quad (2.11)$$

hence

$$\boldsymbol{\alpha} = \mathbf{A}^{-1}\mathbf{b}$$

Note that the above presented discrete Galerkin method of evaluation of optimal $\boldsymbol{\alpha}$ also provides minimum of the quadratic error of $\boldsymbol{\varepsilon}$ in the \mathcal{R}^m space $\mathbf{l} = \boldsymbol{\varepsilon}^\top \boldsymbol{\varepsilon}$

$$\mathbf{l} = \boldsymbol{\varepsilon} \boldsymbol{\varepsilon}^\top = [\mathbf{v} - \mathbf{V}^\top \boldsymbol{\alpha}]^\top [\mathbf{v} - \mathbf{V}^\top \boldsymbol{\alpha}] = [\mathbf{v}^\top - \boldsymbol{\alpha}^\top \mathbf{V}][\mathbf{v} - \mathbf{V}^\top \boldsymbol{\alpha}] \quad (2.12)$$

The stationary condition $\partial \mathbf{l} / \partial \boldsymbol{\alpha} = \mathbf{0}$, provides a set of n linear equations (2.9) and (2.11).

3. Verification of the method

In engineering practice, the number of measurements of imperfections is limited. Moreover, patterns of imperfections, which are most important for future stability analyses, are not *a priori* known. Hence, we face a difficulty that the measurements of imperfections in situ are not only limited, but often not in optimal points of the structure. Therefore, the proper calibration of scale factors α_i plays the important role. The proposed method makes it possible to represent the imperfections as a linear superposition of a limited number of such eigenmodes which play the crucial role in stability of the structure. It is particularly important in the class of stability problems when two or more eigenvalues, which correspond with local and global buckling, coincide or are close to each other. This interactive buckling is typical for thin-walled structures under consideration and is usually connected with high sensitivity to imperfections.

The method of developing the imperfections in series of eigenmodes computed from the linear stability problem is aimed at complex nonlinear stability analysis accounting for initial imperfections. However, for the sake of simplicity, let us start the considerations from the Euler column (Fig. 1).

The buckling modes are

$$u_i = \sin i\pi x \quad (3.1)$$

where $x = [0, 1]$ is the non-dimensional coordinate measured along the length of the column. Through the examples, we will study, verify and validate the proposed algorithm.

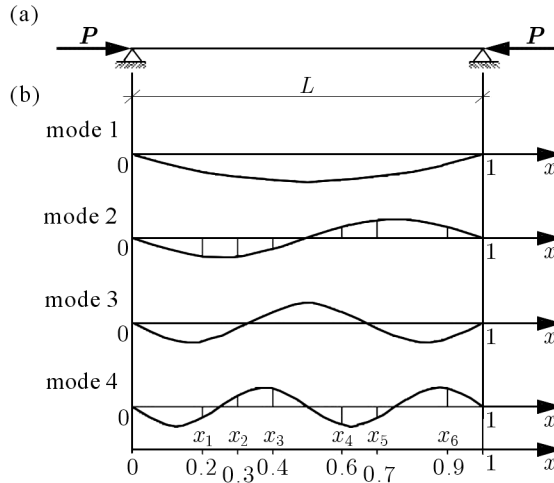


Fig. 1. Simply supported, axially loaded column: (a) geometry, (b) buckling modes. Coordinates x_1, \dots, x_6 indicate points of simulated imperfections

3.1. Example 1

In order to check the correctness of the proposed method, let us assume that the measured imperfection corresponds with the second and fourth buckling mode with amplitudes α^0 equal to 0.03 and 0.07, respectively. Let the imperfections be measured in $m = 6$ points, placed along the column at $x_k = 0.2, 0.3, 0.4, 0.6, 0.7, 0.9$. The measured imperfection vector \mathbf{v} is

$$\begin{aligned} \mathbf{v} &= [u(x_k)] = [0.03 \sin 2\pi x_k + 0.07 \sin 4\pi x_k] = \\ &= [6.97, -1.26, -4.89, 4.89, 1.26, -8.42] \cdot 10^{-2} \end{aligned} \quad (3.2)$$

The imperfection pattern will be approximated using only four eigenmodes, $n = 4$. The discrete representation of the test function \mathbf{u}_i at $k = 1, \dots, m$ points of measurement of the imperfections can be calculated as

$$\begin{aligned} \mathbf{V} &= [V_{ik}] = [u_i(x_k)] = [\sin i\pi x_k] = \\ &= \begin{bmatrix} 58.78 & 80.90 & 95.11 & 95.11 & 80.90 & 30.90 \\ 95.11 & 95.11 & 58.78 & -58.78 & -95.11 & -58.78 \\ 95.11 & 30.90 & -58.78 & -58.78 & 30.90 & 80.90 \\ 58.78 & -58.78 & -95.11 & 95.11 & 58.78 & -95.11 \end{bmatrix} \cdot 10^{-2} \end{aligned} \quad (3.3)$$

Matrices \mathbf{A} and \mathbf{b} are

$$A_{ij} = A_{ji} = \sum_{k=1}^{m=6} u_i(x_k)u_j(x_k) \tag{3.4}$$

$$\mathbf{A} = \begin{bmatrix} 3.59017 & 0.37738 & 0.19098 & 0.01599 \\ 0.37738 & 3.75 & 0.42898 & -1.11804 \\ 0.19098 & 0.42898 & 2.440983 & -0.21041 \\ 0.05199 & -1.11804 & -0.21041 & 3.75 \end{bmatrix}$$

and

$$b_j = \sum_{k=1}^{m=6} u_j(x_k)u(x_k) \qquad \mathbf{b} = \begin{bmatrix} 0.01493336 \\ 0.03423762 \\ -0.00185886 \\ 0.22895898 \end{bmatrix} \tag{3.5}$$

hence

$$\boldsymbol{\alpha} = \mathbf{A}^{-1}\mathbf{b} = \begin{bmatrix} \alpha_1 \\ \alpha_2 \\ \alpha_3 \\ \alpha_4 \end{bmatrix} = \begin{bmatrix} 0 \\ 0.03 \\ 0 \\ 0.07 \end{bmatrix} \tag{3.6}$$

As a result, the expected exact value of α is obtained.

Several other testing examples were solved for different numbers of measurement points and test functions. However, in order to check the correctness of the method, in all those examples, idealized patterns of imperfections were introduced. They took the form of linear combinations of such eigenmodes which were used as test functions in the approximation. No wonder that the examples demonstrated that the exact approximation was always obtained in cases when the number of measurements m was equal or greater than the number of test functions n . This is illustrated in Table 1.

The error of approximation can be calculated in the space L^2

$$\|\tilde{u}(x) - u(x)\|_{L^2} = \sqrt{\int_0^1 \varepsilon^2 dx} = \sqrt{\int_0^1 \sum_i [\alpha_i \tilde{u}_i(x) - u(x)]^2} \tag{3.7}$$

Basing on the orthogonality of eigenmodes, the error (Eq. (3.7)) takes the form

$$\|\tilde{u}(x) - u(x)\|_{L^2} = \sqrt{\int_0^1 \left[\sum_{i=1}^4 (\alpha_i - \alpha_i^0)^2 \sin^2 i\pi x \right] dx} \tag{3.8}$$

Table 1. Error of the approximation for different numbers and distributions of points of simulated measurements

No.	No. of measurement points m	Points of measurements	Approximated values α	Error of approxim. in space L^2
1.	6	$x_k = 0.2, 0.3, 0.4, 0.6, 0.7, 0.8$	$\alpha_1 = 0.0, \alpha_2 = 0.03, \alpha_3 = 0.0, \alpha_4 = 0.07$	0.0
2.	6	$x_k = 0.1, 0.2, 0.3, 0.4, 0.5, 0.55$	$\alpha_1 = 0.0, \alpha_2 = 0.03, \alpha_3 = 0.0, \alpha_4 = 0.07$	0.0
3.	4	$x_k = 0.2, 0.3, 0.4, 0.6$	$\alpha_1 = 0.0, \alpha_2 = 0.03, \alpha_3 = 0.0, \alpha_4 = 0.07,$	0.0
4.	4	$x_k = 0.5, 0.6, 0.7, 0.8$	$\alpha_1 = -5.54 \cdot 10^{-15}$ $\alpha_3 = -4.02 \cdot 10^{-15}$ $\alpha_2 = 0.03, \alpha_4 = 0.07$	0.0
5.	3	$x_k = 0.1, 0.2, 0.3$	$\alpha_1 = 0.057, \alpha_2 = -0.01,$ $\alpha_3 = 6.09 \cdot 10^{-3},$ $\alpha_4 = 0.068$	$3.82 \cdot 10^{-2}$
6.	3	$x_k = 0.2, 0.3, 0.4$	$\alpha_1 = -0.034, \alpha_2 = 0.067,$ $\alpha_3 = -0.019, \alpha_4 = 0.075$	$1.05 \cdot 10^{-2}$

Note that in the above idealized example the distribution of simulated measurement points did not affect the result of the approximation, provided that $m \geq n$.

In the next examples presented in the paper, a more general pattern of imperfections will be used.

3.2. Example 2

Following example 1, we use the first four buckling modes (3.1) in the series approximating the imperfection pattern. However, we assume now that the imperfections correspond with the second, fourth and seventh buckling mode with amplitudes α^0 equal to 0.03, 0.07 and 0.01, respectively. It means that the seventh buckling mode with a multiplier 0.01 is superposed on the imperfection pattern from example 1.

Let the imperfections be measured in $m = 6$ points, placed along the column at $x_k = 0.2, 0.3, 0.4, 0.6, 0.7, 0.9$. Now, the assumed imperfection vector \boldsymbol{v} is

$$\begin{aligned} \mathbf{v}^\top &= [u(x_k)] = [0.03 \sin 2\pi x_k + 0.07 \sin 4\pi x_k + 0.01 \sin 7\pi x_k] = \\ &= [6.0, -0.9523, -4.3, 5.5, 1.6, -7.6] \cdot 10^{-2} \end{aligned} \tag{3.9}$$

Following the presented above algorithm, we obtain the approximated values of α

$$\alpha = \mathbf{A}^{-1}\mathbf{b} = \begin{bmatrix} \alpha_1 \\ \alpha_2 \\ \alpha_3 \\ \alpha_4 \end{bmatrix} = \begin{bmatrix} 0.0045 \\ 0.025 \\ 0.0029 \\ 0.065 \end{bmatrix} \tag{3.10}$$

Now, the approximated imperfection vector $\tilde{\mathbf{v}}$ is

$$\begin{aligned} \tilde{\mathbf{v}}^\top &= [u(x_k)] = [\alpha_2 \sin 2\pi x_k + \alpha_4 \sin 4\pi x_k + \alpha_7 \sin 7\pi x_k] = \\ &= [5.247, -1.134, -4.125, 5.30, 1.752, -6.842] \cdot 10^{-2} \end{aligned} \tag{3.11}$$

The error of approximation in the space L^2 is

$$\sqrt{\int_0^1 \left[\sum_{i=1}^4 (\alpha_i - \alpha_i^0)^2 \sin^2 i\pi x + (\alpha_7 - \alpha_7^0)^2 \sin^2 7\pi x \right] dx} = 4.99 \cdot 10^{-2} \tag{3.12}$$

where according to the assumption $\alpha_1^0 = \alpha_3^0 = \alpha_{+7} = 0$, $\alpha_2^0 = 0.03$, $\alpha_4^0 = 0.07$, $\alpha_7^0 = 0.01$.

The exactness of approximation can be checked using the mean quadratic error in the \mathcal{R}^6 space

$$\varepsilon_{average}^2 = \frac{1}{m} \sum_{i=1}^m (\tilde{\mathbf{v}}_i - \mathbf{v}_i)^2 = 2.2 \cdot 10^{-5} \tag{3.13}$$

The effectiveness of approximation was analysed for different numbers m and various distributions x_k of points of simulated measurements. It was demonstrated that the number and distribution of measurement points can strongly affect the error of approximation. This is illustrated in Table 2.

In examples 1 and 2, we considered discrete representations of the imperfection pattern. Note that in the case of a continuous representation of the imperfection pattern in the form of a sine series, the variation of imperfection by superposition of the seventh mode could not be captured using a series limited to four terms, because this variation is orthogonal to each of the four modes.

Table 2. Error of the approximation for different number and distribution of points of simulated measurements

No.	No. m of mea- surem.	Points of measurements x_k	Approximated values α	Error of approximation	
				in L^2	$\alpha_{average}^2$
1.	10	$x_k = 0.1, 0.2,$ $0.3, 0.4, 0.5, 0.6,$ $0.7, 0.8, 0.9, 0.95$	$\alpha_1 = 0.0, \alpha_2 = 0.03,$ $\alpha_3 = 0.0, \alpha_4 = 0.07$	0.0	0.0
2.	9	$x_k = 0.1, 0.2,$ $0.3, 0.4, 0.5, 0.6,$ $0.7, 0.8, 0.9$	$\alpha_1 = 0.0, \alpha_2 = 0.03,$ $\alpha_3 = 0.0, \alpha_4 = 0.07$	0.0	0.0
3.	8	$x_k = 0.2, 0.3,$ $0.4, 0.5, 0.6, 0.7,$ $0.8, 0.9$	$\alpha_1 = 8.333 \cdot 10^{-4},$ $\alpha_2 = 0.028,$ $\alpha_3 = -2.182 \cdot 10^{-3},$ $\alpha_4 = 0.067$	$4.96 \cdot 10^{-2}$	$6.096 \cdot 10^{-6}$
4.	4	$x_k = 0.2, 0.3,$ $0.4, 0.6$	$\alpha_1 = 0.017,$ $\alpha_2 = -2.064 \cdot 10^{-3},$ $\alpha_3 = 0.018,$ $\alpha_4 = 0.053$	$5.30 \cdot 10^{-2}$	$1.57 \cdot 10^{-4}$
5.	3	$x_k = 0.2, 0.3, 0.4$	$\alpha_1 = -0.017,$ $\alpha_2 = 0.04,$ $\alpha_3 = -2.39 \cdot 10^{-3},$ $\alpha_4 = 0.058$	$1.64 \cdot 10^{-2}$	$1.93 \cdot 10^{-4}$

3.3. Example 3

Assume now that the simulated measurements are contaminated with a white noise produced by $m = 6$ independent sources, each with a random output following a uniform distribution between -0.5 and 0.5 .

Now, we assume the basic imperfection vector \mathbf{v}^0 to be similar to \mathbf{v} from example 1

$$\begin{aligned} \mathbf{v}^0 &= [u(x_k)] = [0.03 \sin 2\pi x_k + 0.07 \sin 4\pi x_k] = \\ &= [6.97, -1.26, -4.89, 4.89, 1.26, -8.42] \cdot 10^{-2} \end{aligned} \quad (3.14)$$

The random generator of the white noise produced the vector

$$\mathbf{whiten}(6)^\top = [-0.499, -0.307, 0.085, -0.15, 0.323, -0.326] \quad (3.15)$$

Assume a white noise amplitude $c = 0.2$. The output vector \mathbf{v} is

$$\mathbf{v}^n = \mathbf{whiten}(6)c \tag{3.16}$$

The imperfection vector with the white noise can be expressed as

$$\mathbf{v}^\top = [\mathbf{v}^0 + \mathbf{v}^n]^\top = [7.3, -2.0, -5.8, 3.9, 1.6, -7.6] \cdot 10^{-2} \tag{3.17}$$

Approximated components of the vector $\boldsymbol{\alpha}$ are

$$\boldsymbol{\alpha} = \mathbf{A}^{-1}\mathbf{b} = \begin{bmatrix} \alpha_1 \\ \alpha_2 \\ \alpha_3 \\ \alpha_4 \end{bmatrix} = \begin{bmatrix} 0.004667 \\ 0.026 \\ 0.009102 \\ 0.066 \end{bmatrix} \tag{3.18}$$

Now, the approximated imperfection vector $\tilde{\mathbf{v}}$ is

$$\tilde{\mathbf{v}} = [7.3, -1.6, -5.4, 5.4, 1.6, -8.9] \cdot 10^{-2} \tag{3.19}$$

The mean quadratic error in the \mathcal{R}^6 space can be calculated according to the following formula

$$\frac{1}{m} \sum_{i=1}^m (\tilde{v}_i - v_i)^2 = 5.299 \cdot 10^{-6} \tag{3.20}$$

The error of approximation for different values of the white noise amplitude c is presented in Fig. 2.

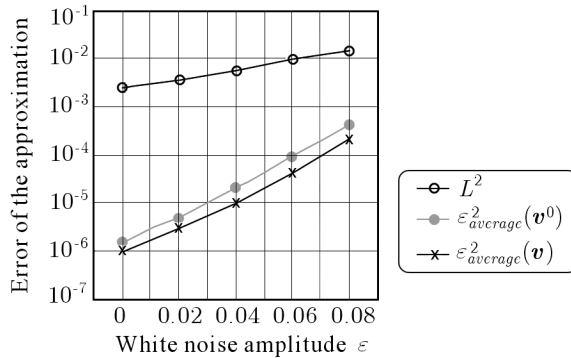


Fig. 2. The mean quadratic error for different values of the white noise amplitude c

4. Measurement of actual imperfections

In this Section the actual imperfections of steel thin-walled cold-formed profiles are discussed. The measurements were performed on sigma sections 300 mm high with walls 1.5 mm thick ($\Sigma 300 \times 1.5$), shown in Fig. 3a.

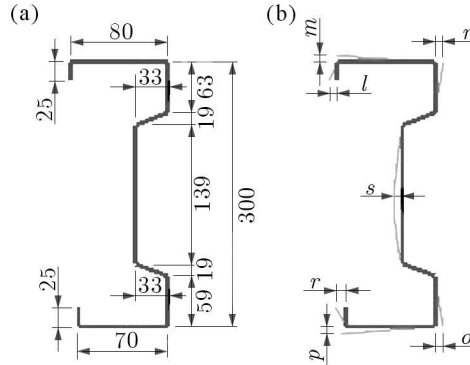


Fig. 3. Profile $\Sigma 300 \times 1.5$ (a) design dimensions, (b) measured dimensions

Eighteen members were examined and initial local-sectional geometric imperfections were identified. Thickness and width of all walls of the cross-section and variations of the contour were measured in 5 cross-sections along the length of the members. A statistical data processing of the measured values was performed. The Gauss distribution and the confidence level 95% were assumed. Thus, we arrived at the limit values

$$a_{lower/upper} = a_{mean} \mp 1.64\sigma \quad (4.1)$$

where σ is the standard deviation of a . The limit values of imperfections are

$$\delta a_{min/max} = a_{lower/upper} - a_{design} \quad (4.2)$$

The results are presented in Table 3. The rows *a-h* refer to width of the walls, whereas the next rows describe deformations of the contour. The limit values of imperfections are presented in columns 5 and 6.

The design cross-sectional dimensions are shown in Fig. 3a. All these dimensions were compared with actual values measured in situ and thus the dimensional imperfections were evaluated. Figure 3b shows the next class of measured imperfections, namely shape imperfections. Table 3 presents the results of statistical processing of all design and shape imperfections.

Table 3. Profile $\Sigma 300 \times 1.5$. Values of imperfections in mm

Symbol	Design dimension	Arithmetic mean	Standard deviation	Maximum imperf.	Minimum imperf.
1	2	3	4	5	6
<i>a</i>	25.00	28.61	1.98	6.86	0.37
<i>b</i>	80.00	80.89	1.09	2.67	-0.89
<i>c</i>	63.50	63.97	1.36	2.70	-1.75
<i>d</i>	19.00	17.24	1.84	1.26	-4.77
<i>e</i>	139.00	138.64	0.88	1.08	-1.80
<i>f</i>	19.00	17.55	1.59	1.16	-4.06
<i>g</i>	59.50	60.50	1.32	3.16	-1.17
<i>h</i>	70.00	70.39	1.31	2.55	-1.76
<i>l</i>	0.00	0.00	1.10	1.80	-1.80
<i>m</i>	0.00	0.17	1.58	2.77	-2.43
<i>n</i>	0.00	0.11	1.65	2.82	-2.59
<i>o</i>	0.00	-0.14	1.17	1.78	-2.07
<i>p</i>	0.00	-0.06	1.29	2.06	-2.19
<i>r</i>	0.00	-0.11	1.25	1.95	-2.16
<i>s</i>	0.00	0.01	0.73	1.20	-1.18

The shape imperfections can be classified as symmetric "opening" (SO), symmetric "closing" (SC) or asymmetric deformation (AS). They are presented in Fig. 4. These three forms of local imperfections appeared periodically throughout the length of elements, which suggests that they originated in the cold-forming process.

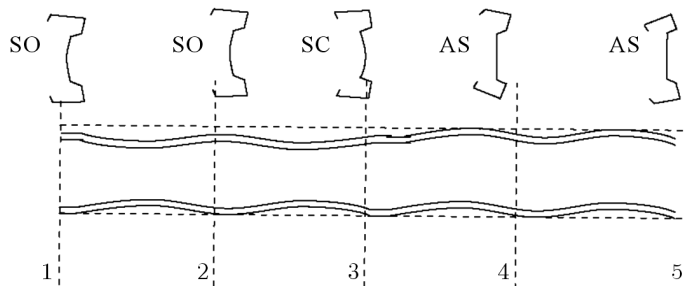


Fig. 4. Demonstrative imperfection patterns along the Σ members

The average values of shape imperfections *l-s* in different cross sections *x* are presented in Fig. 5. These values can be used as coordinates v_k of the vector \mathbf{v} to calculate scale factors α_i in series (1) using equation (2.12).

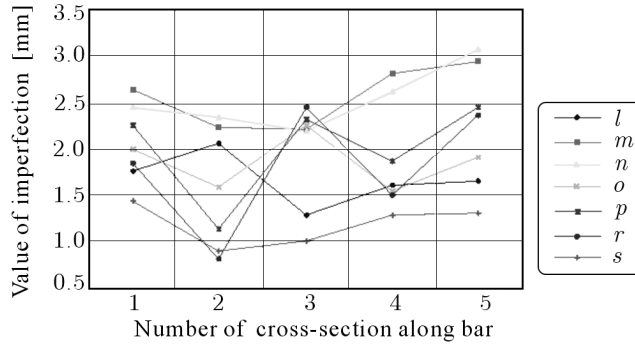


Fig. 5. Spectrum of average shape imperfections in a bar

5. Eigenvalue problem

The eigenvectors $u_i(x)$ representing the buckling mode are computed from the linear eigenvalue problem

$$(\mathbf{K}^0 + \lambda \mathbf{K}^G) \mathbf{U} = \mathbf{0} \quad (5.1)$$

where \mathbf{K}^0 denotes the small-displacement stiffness matrix, \mathbf{K}^G is the geometric stiffness matrix, λ is the load multiplier and the eigenvectors \mathbf{U} represent the buckling mode shapes.

Numerical examples were solved using the general purpose finite element program ABAQUS. A simply supported axially loaded column was analysed. To consider local imperfections presented in Section 4, local buckling modes had to be captured. Therefore, four-node doubly curved shell elements with reduced integration were employed. In the FEM 2D model, the boundary conditions were introduced so as to represent a spherical hinge support. Hence, in all nodes of the boundary cross-section, displacements in the direction x (longitudinal axis of the column) were unconstrained except for the center point at one support. The transversal displacements at the supports were assumed to be zero. Nodal forces were applied at the boundary cross-section in the longitudinal direction x with the magnitude σ_x representing the force P .

Assume the length of the axially compressed column to be 4.0 m. Five different eigenmodes were extracted from linear stability analysis. During the analysis, from the eigenvectors $u_i(x)$, the matrix \mathbf{V}_{ik} representing the buckling mode at the points of measurement was calculated. Figure 6 shows the shapes of buckling modes related to the lowest eigenvalues. The next eigenvalues were much higher. Since the first three eigenvalues are close to each other, at least these three eigenmodes should be used in the series approximating the

initial imperfection pattern. However, for better illustration of the interaction of global and local imperfections, in the following example we will use only the first two eigenmodes. Mode 1 is a global one and mode 2 represents a local buckling form.

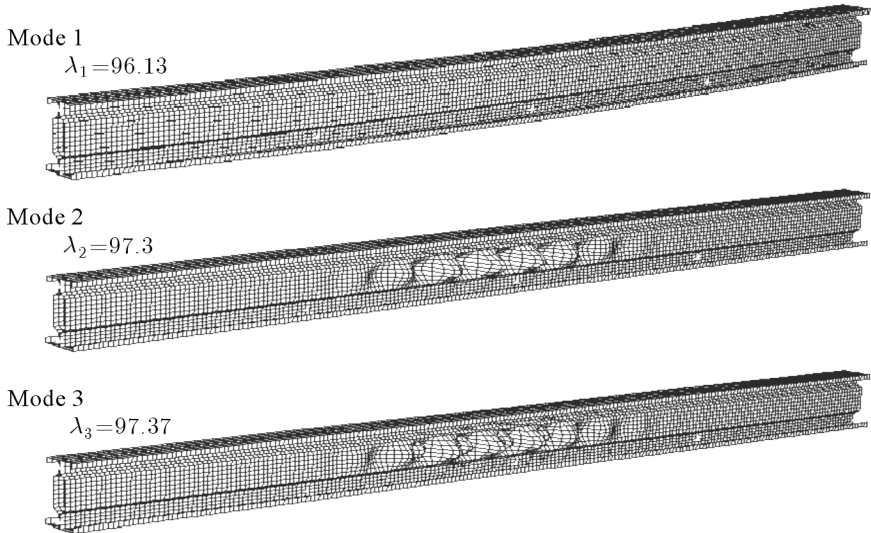


Fig. 6. Shapes of buckling modes for $2 \times \Sigma$ column

Since λ_1 is close to λ_2 , an interactive buckling can appear. Hence, we can expect unstable postbuckling behavior, reduction of load capacity and sensitivity to imperfections. To study this issue, we will carry out a nonlinear stability analysis allowing for different kinds of initial geometric imperfections, global, local and global/local.

6. Nonlinear stability analysis

The imperfections were introduced into stability analysis by perturbing the initial geometry by imperfections in the form of Eqs. (2.1) and (2.2). Our objective is to study the influence of actual magnitudes of global and local imperfections. Therefore, the proportionality factor associated with global buckling mode 1 in Fig. 6 has been assumed $\alpha_1 = 4$, thus modeling the global imperfection amplitude to be in accordance with the design code provisions referring to allowable execution tolerances. The scale factor for local mode 2 has been

evaluated as $\alpha_2 = 2.04$, using the procedure described in Section 2 and basing on measurements described in Section 4.

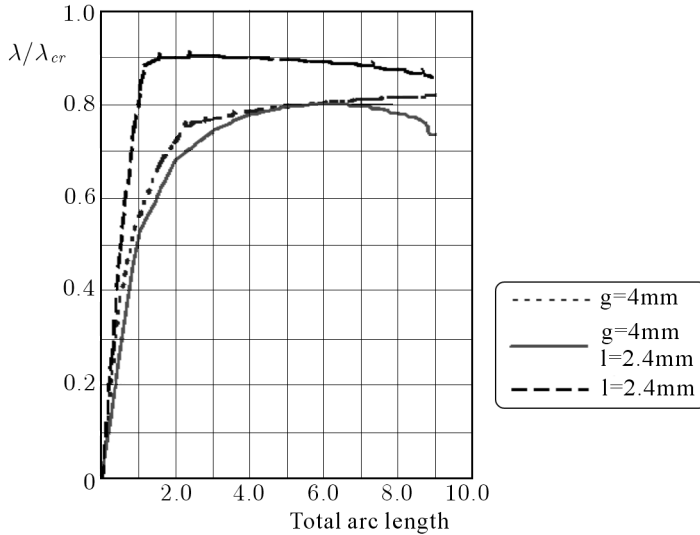


Fig. 7. Load proportionality factor for the column made of 2Σ with different shapes of imperfections

Figure 7 shows plots of the load proportionality factor λ/λ_{cr} versus the total arc length in the Riks algorithm, where λ_{cr} is the critical load factor for the ideal column with perfect geometry obtained from linear stability analysis. The plots in Fig. 7 refer to global (g), local (l) and global-local (g+l) shapes of imperfections. As expected, for the global imperfections, the post buckling path is stable, however the maximum load capacity is reduced by 20% in relation to λ_{cr} . Conversely, for local imperfections, the maximum load is reduced only by 10% but the post buckling is unstable. The interaction of global and local imperfections represents the worst case when the post buckling path is unstable and 20% reduction of maximal load is observed.

7. Concluding remarks

In the paper, the modeling of initial geometrical imperfections in stability analysis was presented. Local sectional imperfections of cold-formed thin-walled steel sigma cross-section had been measured in situ. The measured values were then subjected to statistical processing.

The paper presents a method of modeling initial imperfections. The imperfections are modeled in the form of a displacement vector with the dimension and physical meaning adequate to the displacement vector in the FEM model of the structure. The vector of initial imperfections is assumed in the form of a series of a limited number of eigenfunctions obtained from linear stability analysis. Such representation of imperfections makes it easy to employ FEM in non-linear stability analysis. The scale coefficients in the series were evaluated basing on measurements and using the discrete Galerkin approach, thus providing the minimum of discrepancy between the measured values of initial imperfections and their approximated representation. The method was verified by making use of idealized examples and examples where idealized simulated measurements were contaminated with a white noise.

The stability analysis of a column made of a cold-formed thin-walled steel sigma cross-section was carried out. Particular attention was paid to the interaction of global and local buckling which can result in excessive sensitivity to imperfections and in unstable behavior. It was found that the initial sectional imperfections did not remarkably reduce the maximum bearing capacity of the column, but they made the post buckling behavior unstable.

References

1. ABAQUS/Standard, Hibbitt, Karlsson & Sorensen, Inc., 2001
2. CHROŚCIELEWSKI J., LUBOWIECKA I., SZYMCZAK C., 2006, On some aspects of torsional buckling of thin-walled I-beam columns, *Computers and Structures*, **84**, 1946-1957
3. DUBINA D., UNGUREANU V., SZABO I., 2001, Codification of imperfections for advanced finite analysis of cold-formed steel members, *Proceedings of the 3rd ICTWS 2001*, 179-186
4. FANG Y., PEKOZ T., 2001, Design of cold-formed steel plain channels, *School of Civil and Environmental Engineering Report*, Cornell University, Ithaca
5. GARSTECKI A., KAKOL W., RZESZUT K., 2002, Classification of local-sectional geometric imperfections of steel thin-walled cold-formed sigma members, *Foundations of Civil Environmental Engineering*, **45**
6. KAŁOL W., RZESZUT K., GARSTECKI A., 2002, Stability analysis of cold-formed thin-walled members, *Fifth World Congress on Computational Mechanics*, Vienna, Austria

7. LAUBSCHER R.F., 2004, An experimental and numerical investigation of the axial resistance of hot rolled 3CR12 columns, *Proceedings of the Fourth International Conference on Coupled Instabilities in Metal Structures*, Rome, Italy, 411-427
8. LECHNER B., PIRCHER M., 2005, Analysis of imperfection measurements of structural members, *Thin-Walled Structures*, **43**, 361-374
9. SZYMCZAK C., 2006, The effect of nonlinear restraint on torsional buckling and post-buckling behaviour of thin-walled column, *Foundation of Civil and Environmental Engineering*, 333-342

Modelowanie początkowych imperfekcji geometrycznych w zagadnieniach stateczności konstrukcji cienkościennych

Streszczenie

W pracy przedstawiono metodę modelowania początkowych imperfekcji geometrycznych na podstawie rzeczywistych imperfekcji pomierzonych „in situ”. Zaproponowana metoda polega na automatycznym tworzeniu sygnału imperfekcji w postaci serii funkcji własnych uzyskanych z liniowej analizy stateczności. Do modelowania imperfekcji użyto niewielkiej liczby najbardziej niekorzystnych postaci własnych. Efektywność metody analizowano ze względu na liczbę punktów pomiaru oraz sposób ich rozmieszczenia na długości pręta, minimalizując błąd aproksymacji. W dalszej części pracy, proponowana metoda została zastosowana do nieliniowej analizy stateczności z uwzględnieniem imperfekcji prętów cienkościennych typu „ Σ ”. Do rozwiązania problemu nieliniowej analizy stateczności zastosowano metodę Riks’a. Przykłady numeryczne ilustrują wpływ początkowych imperfekcji geometrycznych na pokrytyczne zachowanie konstrukcji.

Manuscript received April 2, 2009; accepted for print April 22, 2009